GEOLOGICA BELGICA (2009) 12/3-4: 145-159

A REGIONAL, S-DIPPING LATE EARLY TO MIDDLE ORDOVICIAN PALAEOSLOPE IN THE BRABANT MASSIF, AS INDICATED BY SLUMP FOLDS (ANGLO-BRABANT DEFORMATION BELT, BELGIUM)

Timothy N. DEBACKER & Els DE MEESTER

(8 figures, 2 tables)

Research Unit Palaeontology, Geology & Pedology, Universiteit Gent, Krijgslaan 281, S8, B-9000 Gent, e-mail: Timothy.Debacker@UGent.be

ABSTRACT. Within the upper Lower to Middle Ordovician directly north of the Quenast plug (Senne valley, Brabant Massif) numerous pre-cleavage folds and associated detachments occur. These folds and the associated detachments are attributed to slumping. On the basis of a combination of a) the mean axis method, b) the separation arc method, c) the axial-planar intersection method and d) the fold hinge azimuth and interlimb angle method a SSE-dipping palaeoslope is inferred from these slump features. This is fully compatible with the palaeoslopes inferred by two previous studies on slump folds in other upper Lower to Middle Ordovician outcrop areas of the Brabant Massif. Combined, the results indicate that during the late Early to Middle Ordovician a regionally persistent S-dipping palaeoslope existed within the southern part of the Brabant Massif, with an along-strike length of at least 30 km. Slumping is attributed to slope failure due to seismic loading by normal faulting related to the separation of Avalonia from Gondwana. In this respect, the regional S-dipping palaeoslope may correspond to bedding tilted by antithetic (N-dipping) lystric faults, or to synthetic (S-dipping) normal fault scarps.

KEYWORDS. Anglo-Brabant Deformation Belt, Avalonia, detachment, Ordovician, slump fold, cleavage/fold relationship

1. Introduction

Legrand (1968) already mentioned the presence of slump folds within the Lower Palaeozoic Brabant Massif and particularly stressed the very common occurrence of slump folds and related features within the deposits of the former "Sm1b" (Legrand, 1968). However, within this unit, now corresponding to the lowermost Ordovician (Tremadoc) Chevlipont Formation, slump folds appear scarce in outcrop (cf. Herbosch *et al*., 1991; Debacker, 2001; Beckers, 2003, 2004; Debacker *et al*., 2003). In outcrop, slump folds appear much more common in the overlying upper Lower Ordovician to Middle Ordovician Abbaye de Villers Formation. Both Debacker (2001; see also Debacker *et al*., 2003) and Beckers (2003, 2004; see also Beckers & Debacker, 2006; cf. Michot, 1977) have demonstrated the common presence of slump folds within the upper Lower to Middle Ordovician Abbaye de Villers Formation. More importantly, on the basis of these slump folds, Beckers (2003, 2004) deduced a S-dipping palaeoslope within the Thyle outcrop area, something which was completely unexpected. The Middle Ordovician to upper Silurian deposits of the Condroz Inlier and the Brabant Massif are considered to have been deposited in one large basin, called the Brabant Basin or Condroz-Brabant Basin (Debacker, 2001; Verniers *et al*., 2002; Vanmeirhaeghe, 2006, 2007; Debacker & Vanmeirhaeghe, 2007). At least during the largest part of the period between the Middle Ordovician and the late Silurian, the area of the Condroz Inlier and the SW-part of the Brabant Massif occupied the shallow parts of this basin, whereas the largest part of the Brabant Massif occupied the deeper parts of this basin (Verniers *et al*., 2002; Vanmeirhaeghe, 2006, 2007). On the basis of palaeocurrent, slump folds and facies changes within the Condroz Inlier and the exposed southern parts of the Brabant Massif, and the relationship of these with palaeogeography and the current outcrop and subcrop appearance of the Brabant Massif, many authors deduced a regionally N-dipping palaeoslope for the Silurian and Ordovician in the southern part of the Brabant Basin (Verniers, 1983; Verniers & Van Grootel, 1991; Louwye *et al*., 1992; Verniers *et al*., 2002; Vanmeirhaeghe, 2006, 2007, Debacker & Vanmeirhaeghe, 2007; cf. Debacker *et al*., 2001). In contrast, however, the observations of Beckers (2003, 2004) suggest that, at least within the Thyle outcrop area, a S-dipping palaeoslope was present during the deposition of the upper Lower to Middle Ordovician Abbaye de Villers Formation. Although also the slump fold geometries at Virginal within the Sennette outcrop area (Debacker, 2001; cf. Debacker *et al*., 2003) are compatible with the conclusions of Beckers (2003, 2004), the question remains whether this Ordovician S-directed palaeoslope is a regional feature or merely a local feature.

In this paper we present data on pre-cleavage folds from the upper Lower to Middle Ordovician of the Quenast area and the resulting implications of these for the Brabant Basin.

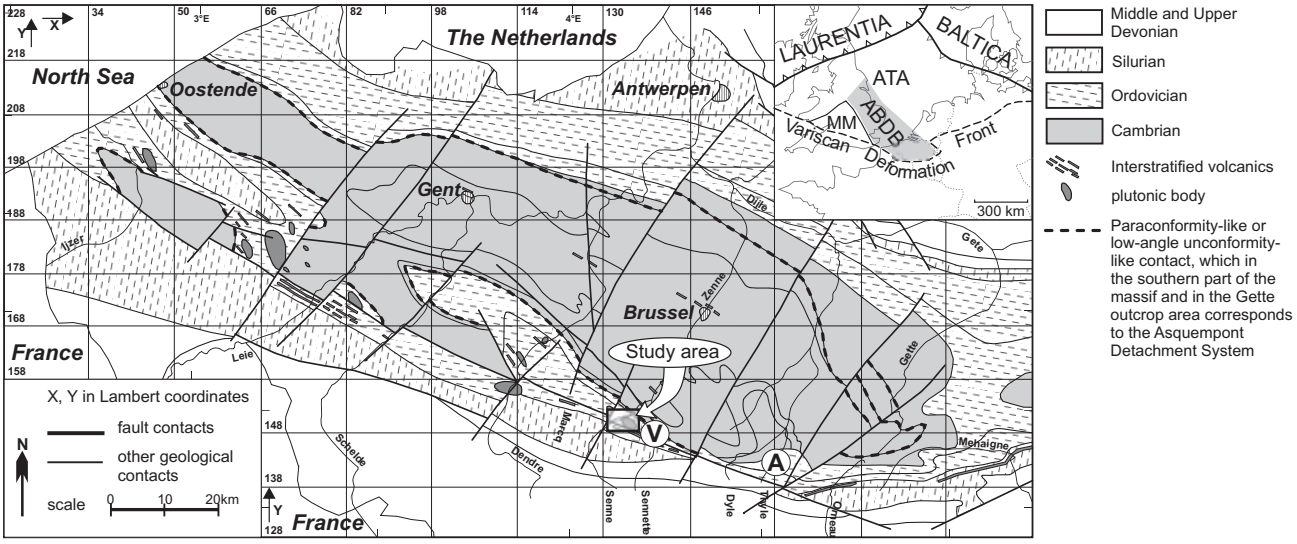

Figure 1: Geological subcrop map of the Brabant Massif, after De Vos *et al.* (1993) and Van Grootel *et al.* (1997), with location of the study area (see also Fig. 2). The upper right inset shows the position of the Brabant Massif within Avalonia (ATA), as the southeastern part of the Anglo-Brabant Deformation Belt (ABDB), flanking the Midlands Microcraton (MM). Also shown is the position of two upper Lower to Middle Ordovician slump fold occurrences, studied previously by Debacker (2001; Debacker *et al*., 2003; V: Virginal) and Beckers (2003, 2004; Beckers & Debacker, 2006; A: Abbey of Villers-la-Ville).

2. Geological setting and lithology

The study area is situated in the Senne outcrop area, one of the classical outcrop areas of the single-phase deformed, Lower Palaeozoic Brabant Massif (Fig. 1). The six studied outcrops, collectively referred to as outcrop Quenast 2 in Debacker & Sintubin (2008), are situated in the northern valley flank of the Senne River, to the north of the Quenast plug, at ~400 to 500 m east of the church of Quenast (Fig. 2). According to the new geological map of Herbosch *et al*. (in press) these outcrops belong to the lower part of the Tribotte Formation, close to the limit with the underlying Abbaye de Villers Formation. Both formations are difficult to distinguish, both lithologically and biostratigraphically, and several authors have even incorporated the deposits of these two formations into one informal unit, named the "Quenast formation" (André *et al*., 1991; Servais *et al*., 1993) or the "Quenast unit" (Lenoir, 1987; Debacker, 2001). As far as the authors are aware of, currently only A. Herbosch is able to distinguish both formations on the basis of lithology, and although chitinozoans, and recently also acritarchs, have been found in both formations, the assemblages are often too poor to draw (bio-)stratigraphical conclusions (see Verniers *et al*., 2001 and Vanguestaine, 2008). Moreover, as the transition between both formations is gradual, it is extremely difficult to localise the limit between both formations accurately (A. Herbosch, pers. comm.).

The deposits consist of often bioturbated, centimetric alternations of irregularly laminated, grey to beige, fine-grained sandstone to siltstone and darker grey silty mudstone. The fine-grained sandstone to siltstone beds are often thicker and occur more frequently than the mudstone beds, and may occasionally reach a thickness of

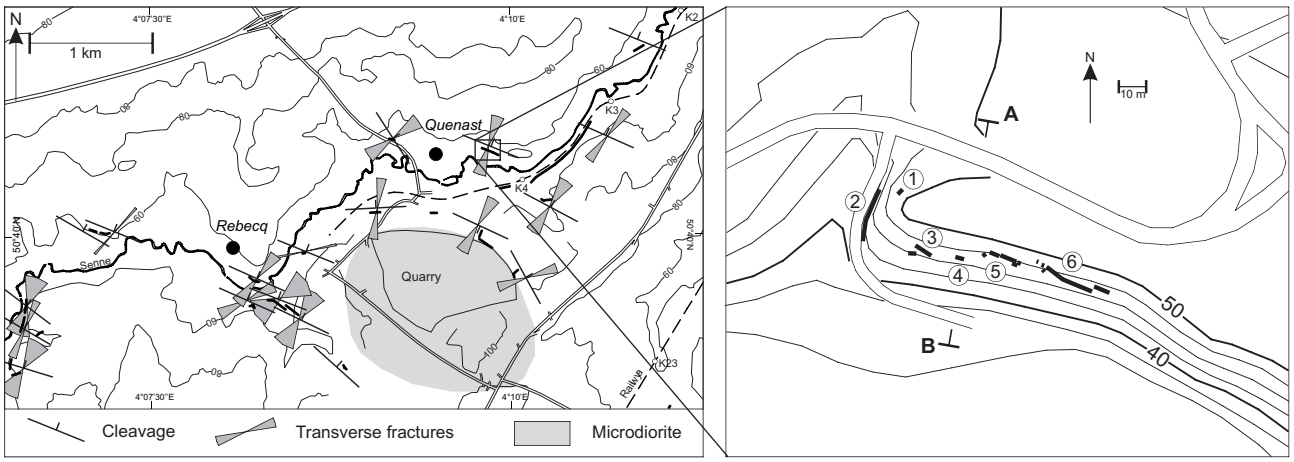

Figure 2: Simplified topographic map of the Rebecq – Quenast area (after Debacker & Sintubin, 2008), with blow-up showing the position of the six outcrops studied. A and B indicate position of section line of Fig. 7.

several dm. Locally, these beds may show large-scale cross-bedding (cf. Herbosch & Lemonne, 2000; Herbosch *et al.*, in press). The silty mudstone beds are usually restricted to cm-thick interbeds between the fine-grained sandstone to siltstone beds. Locally, however, zones occur in which silty mudstone is the dominant lithology. The limits between individual beds may be sharp or diffuse. In the former case, the weathered outcrop surface directly reflects the bedding trace, whereas in the latter, diffuse case, bedding often becomes difficult to trace. Moreover, along strike, the contacts between individual beds may gradually change from sharp to diffuse, and along strike some beds may even become lenticular and seemingly terminate or disappear in zones of disrupted sediments, often with a breccia-like appearance. In addition, the study of the bedding geometry is rendered difficult by the very common occurrence of faults, often oriented at low angles to bedding, and by the presence of relatively small-scale folds of various shapes and styles.

3. Structural field observations

3.1. Cleavage/fold relationship

Individual folds

A large number of folds occur. A summary of the cleavage and fold orientation data can be found in Table 1.

Individual fold hinges have been observed in outcrops 2, 3, 4 and 6. These folds have rather small half wavelengths, never exceeding two metres, and sub-horizontal to gently plunging fold hinge lines. A marked variation in plunge direction is observed (Fig. 3, Table 1). A very characteristic feature of these folds is their restricted occurrence in specific levels, bounded above and below by relatively undeformed planar beds (Figs 4 & 5). In the present context, "relatively undeformed" implies being cleaved and usually tilted but without being folded by the directly underlying or overlying folds. Below, and in Tables 1 & 2, the relatively undeformed beds are referred to as regular bedding.

The small-scale folds have a very pronounced asymmetry, and their axial surfaces are usually at small angles to the overlying and underlying regular bedding. The folds surrounded by a subvertical regular bedding (outcrop 2; Fig. 4, Fig. 6A) have a north-side-up asymmetry or Z-shaped asymmetry when looking east. In outcrops with a gently dipping to subhorizontal regular bedding (e.g. outcrop 3, outcrop 6; Fig. 5, Figs 6B-6G) the folds usually have a top-to-the-south asymmetry or Z-shaped asymmetry when looking east. Noteworthy, in the gently dipping beds of outcrop 6 two adjacent folds show a contrasting, top-to-the-north asymmetry or S-shaped asymmetry when looking east (folds 13 and 14; Fig. 5).

In many folds, a clear mismatch occurs between the orientation of the fold axial surface and the orientation of cleavage (folds 1, 2, 6, 12, 13, 14; Figs 4, 5, 6A, 6B & 6C). In these folds, cleavage was observed to cross-cut the fold axial surface and the fold limbs, hereby showing an identical sense of cleavage refraction in opposite fold limbs (e.g. folds 6 & 12). Other folds have an axial surface with approximately the same orientation as the mean cleavage (folds 3-5, 7-10; Figs 5, 6D, 6E & 6F). In detail, however, also in some of these folds cleavage was observed to crosscut the axial surface and the fold limbs at a relatively small angle, locally showing the same sense of cleavage refraction in opposite fold limbs (e.g. folds 7, 8, 16; Figs 5, 6D & 6E).

In outcrop 5, bedding orientation changes from moderately S-dipping in the top parts of the outcrop to steeply S-dipping in the bottom parts, with a mean bedding orientation of ~50°S. This reflects the presence of an antiform with a subhorizontal fold axis and with a top-to-the-south asymmetry or Z-shaped asymmetry when looking east. This fold, of which the hinge could not be observed, differs from the other folds in the fact that 1) both the amplitude and the half wavelength are larger, and 2) no truncation by underlying or overlying regular bedding could be observed.

Regular bedding and cleavage orientation

On the basis of the regular bedding orientation, three groups of outcrops can be distinguished. Outcrops 1, 3, 4 and 6 are characterised by subhorizontal to gently

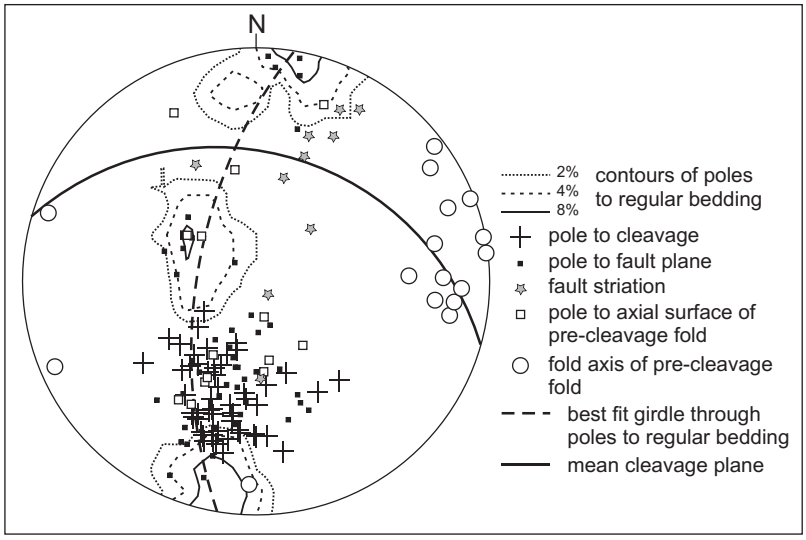

Figure 3: Lower-hemisphere equal area projection with data from the six studied outcrops, showing contours of poles to regular bedding, poles to cleavage, poles to pre-cleavage fold axial surfaces, pre-cleavage fold axes, poles to fault planes, fault striations, the best fit girdle through pole to regular bedding, and the mean cleavage plane.

Outcrop	Fold	Mean regular bedding	Fold B-axis	Fold axial surface	Cleavage (S1)	Fold interlimb angle	Relationship of fold with S1
1	/	015/24E (n=4)	/	/	315/39NE (n=3)	/	/
2	1	284/85N (n=47)	07/288 (n=13)	111/70S	279/53N (n=19)	80°	Pre-S1
2	2		17/100 (n=6)	079/40S		70°	Pre-S1
3	3	066/13S (n=2)	01/079 (n=4)	261/28N	279/39N (n=5)	70°	Pre- or syn-S1
3	4		01/083 (n=4)	265/32N		80°	Pre- or syn-S1
3	5		07/247 (n=6)	234/28NW		130°	Pre- or syn-S1
4	6	032/28SE (n=8)	14/182 (n=9)	039/25SE	292/38N (n=6)	30°	Pre-S1
5	/	076/53S (n=24)	30/099 (n=24)	/	290/40N (n=1)	/	Syn-S1(?)
6	7	008/16E (n=14)	13/092 (n=6)	300/30NE	292/40N (n=19)	90°	Pre-S1
6	8		21/089 (n=3)	297/40NE		110°	Pre-S1
6	9		16/096 (n=4)	297/38NE		100°	Pre- or syn-S1
6	10		24/096 (n=4)	298/50NE		140°	Pre- or syn-S1
6	11		05/053 (n=4)	/		150°	Pre- or syn-S1
6	12		02/069 (n=6)	258/13N		40°	Pre-S1
6	13		12/057 (n=9)	034/29SE		70°	Pre-S1
6	14		13/069 (n=7)	064/69S		110°	Pre-S1
6	15		23/078 (n=3)	/		150°	Pre- or syn-S1
6	16		35/088 (n=8)	303/51NE		140°	Pre-S1
1-6	/	/	**21/100 (n=99)**	/	**286/44N (n=53)**	**70°**	**Syn-S1**

Table 1: Bedding, cleavage and fold data of the six studied outcrops. The mean regular bedding is the relatively undeformed, more or less uniformly dipping bedding surrounding the small-scale folds. The relationship of the folds with respect to the cleavage is based on cleavage/fold relationships such as cleavage refraction sense, cleavage fanning and axial-planar nature.

S-dipping bedding, whereas outcrop 2, extending for 17 meters across strike, is characterised by an overall subvertical bedding (compare Figs 4 & 5). Outcrop 5 has an intermediate mean bedding orientation (see above).

The mean cleavage dip is similar for outcrops 1, 3, 4, 5 and 6 (see Table 1). In outcrop 2 the mean cleavage dip is significantly steeper. Within the steep beds of outcrop 2 cleavage, dipping less steeply than bedding, shows a Z-shaped cleavage refraction pattern across the more competent beds. In contrast, in the overall gently dipping beds in outcrops 1, 3, 4 and 6, cleavage dips steeper than bedding and shows an S-shaped cleavage refraction pattern across the more competent beds (Figs 4 & 5). Within outcrop 5, cleavage is oriented approximately at right angles to the mean bedding orientation.

3.2. Brittle deformation: faults and related features

Many faults have been observed. In most of the cases these faults occur at relatively low angles to bedding and cleavage. Moreover, in particular in outcrops 3 to 6, usually at least a part of each fault is parallel to the overlying or underlying bedding.

In outcrop 2, oriented at high angles to regional strike, and in which the mean regular bedding is subvertical, most of the faults are moderately to steeply N-dipping (Fig. 4). In contrast, in outcrops 3, 4 and 6 the faults are gently to moderately N- to E-dipping, and occasionally gently S-dipping (Fig. 5). It should be noted that, because of the relative orientation of the outcrops with respect to regional strike, steep E-W-trending faults, as observed in outcrop 2, will be much less obvious in outcrops 3 to 6.

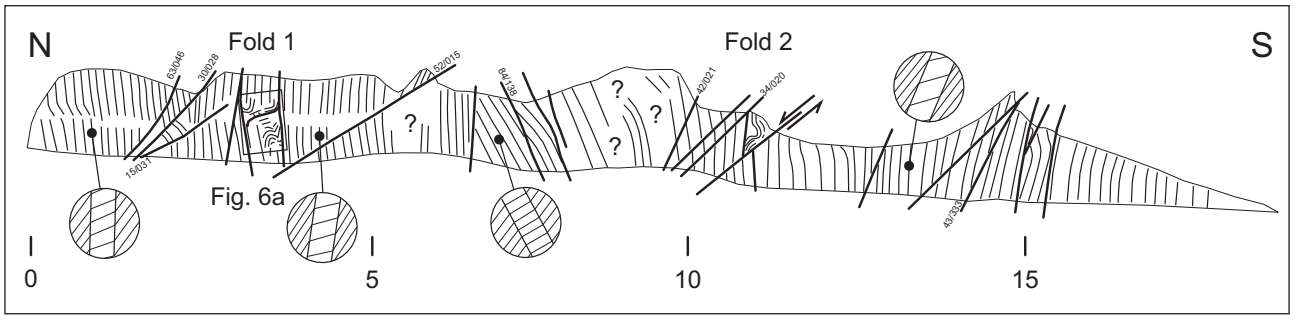

Figure 4: Line drawing of outcrop 2, characterised by an overall steep bedding (thin lines), affected by numerous moderately to steeply dipping faults (thick lines). The overall sense of younging is towards the south. The circular insets schematically show cleavage refraction across a more competent bed in between less competent beds. Where observed, fault striation orientations are given, written as plunge/plunge direction. Sense of fault movement is only shown where known. ?: bedding uncertain or not observed. See Table 1 for orientation data of folds 1 and 2, and Fig. 6A for close-up of fold 1.

However, considering that gently dipping faults, as observed in outcrops 3 to 6, are virtually absent in the steep beds of outcrop 2, a relationship between bedding dip and fault orientation appears to exist for the majority of the faults.

Many of the faults truncate small-scale folds, separating these from the overlying or underlying relatively undeformed regular bedding. In addition, many of the small-scale folds have fold hinge lines with an orientation within the plane of the adjacent faults. Moreover, in particular in outcrop 6, many of these faults have the same curvature as the overlying folded beds (Fig. 5), indicating fault formation prior to or during folding of the overlying beds. Hence, many of the faults appear to show a genetic relationship with the small-scale folds and may in fact have served as detachments during fold development.

Fault striations have only been observed in outcrop 2, in particular on faults which are at relatively high angles to bedding and/or which are not directly adjacent to small-scale folds (Fig. 4). These striations all indicate a dip-slip movement, and plot close to the best fit girdle through the poles to regular bedding (Fig. 3). In most cases, sense of slip could not be determined.

Also on the basis of the macroscopic outcrop appearance, a difference is observed between the subvertical to moderately N-dipping faults in outcrop 2, often oriented at moderate to high angles to bedding, and the faults at low angles to bedding in outcrops 2 to 6. Many of the faults in outcrop 2, in particular those with clear fault striations, are readily apparent in outcrop. These faults contain a centimetric damage zone, and are clearly weathered, resulting in a centimetric depression within the outcrop surface.

In contrast, the majority of the other faults, in particular those in outcrops 3 to 6, do not contain a clear damage zone and often have a welded nature. The latter faults are difficult to recognise and very often their presence is only reflected by sudden bedding truncations. In some cases, these faults juxtapose beds of different orientation. In such cases, unlike bedding orientation, cleavage orientation does not differ on both sides of the faults, implying that cleavage formed after fault-related tilting of the beds (e.g. Figs 6D & 6G).

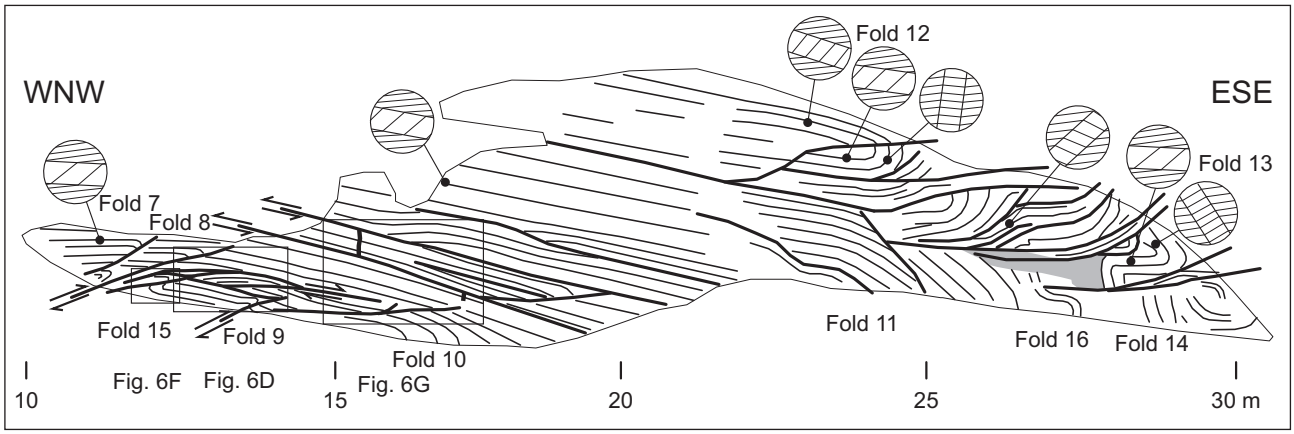

Figure 5: Line drawing of outcrop 6, characterised by an overall subhorizontal to gently dipping bedding (thin lines), affected by numerous small folds and low-angle faults (thick lines). The overall sense of younging is upwards. The circular insets schematically show cleavage refraction across a more competent bed in between less competent beds.
Sense of fault movement is only shown where known. The grey-shaded area represents a zone of pre-cleavage breccia/cataclasite. See Table 1 for fold orientation data and Fig. 6 for close-ups of the areas in the rectangular frames.

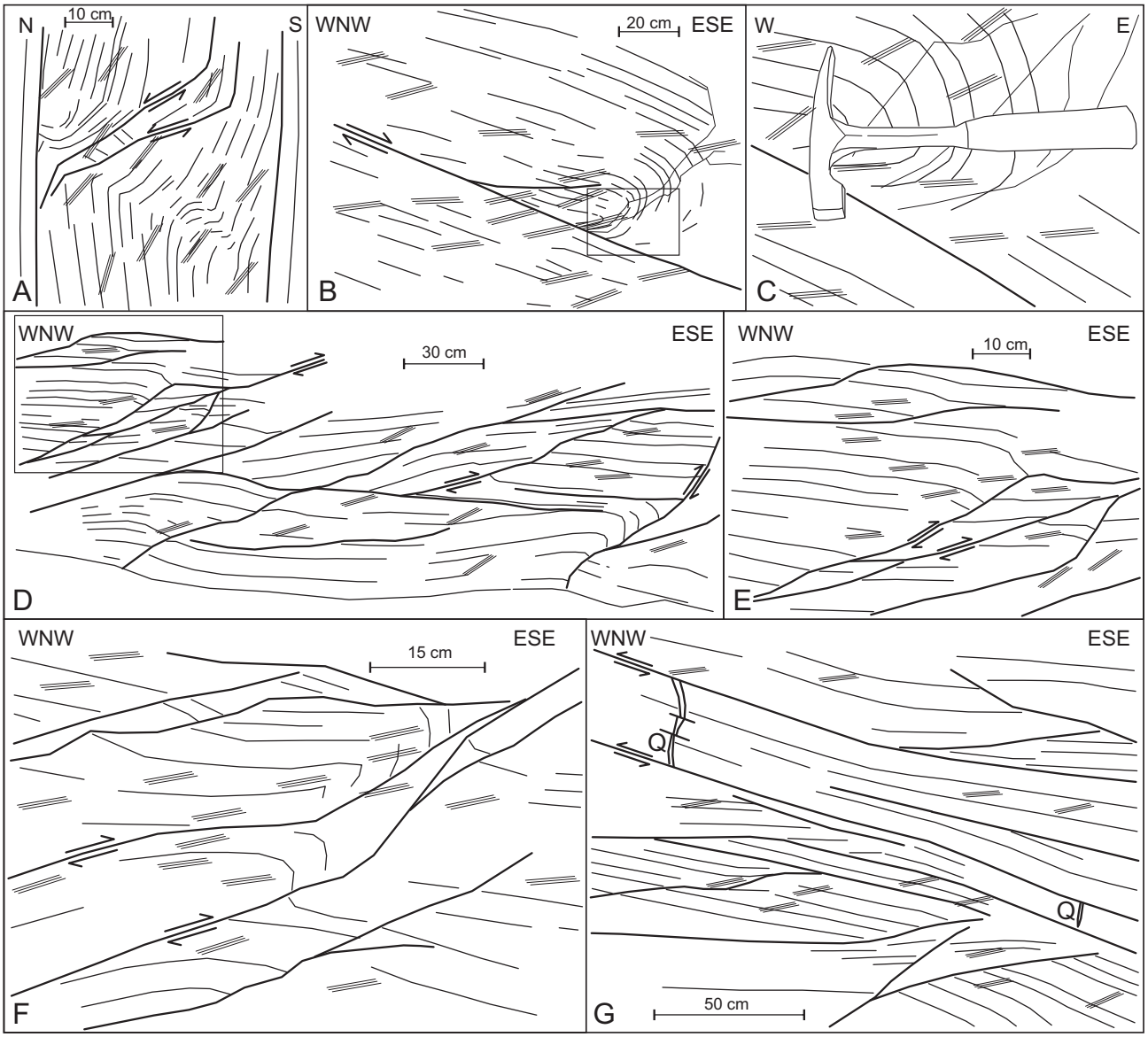

Figure 6: Line-drawings of representative deformation geometries, constructed from traced photographs combined with field sketches. Thick lines represent faults, thinner lines bedding, and groups of three straight thin lines represent cleavage. A) Detailed image of fold 1, with a clear pre-cleavage origin (outcrop 2; see Fig. 4 for position). B) Fold 6, with a clear pre-cleavage origin (outcrop 3); frame indicates position of Fig. 6C. C) Close-up of hinge of fold 6, demonstrating the pre-cleavage nature (outcrop 3; see Fig. 6B for position). D) Folds 8 and 9, and their relationship with small-scale faults oriented at low angles to bedding (outcrop 6; see Fig. 5 for position); frame indicates position of Fig. 6E. E) Close-up of area of fold 8 (see Fig. 6D for position). F) Detailed image of fold 15, and its relationship with small-scale faults oriented at low angles to bedding (outcrop 6; see Fig. 5 for position). G) Subhorizontal to moderately dipping beds affected by numerous low-angle faults, of which two, with a bedding-parallel orientation displace a quartz vein (Q; outcrop 6; see Fig. 5 for position). Note that, like in Fig. 6D, cleavage orientation remains unmodified where bedding orientation changes, implying fault-related tilting of the beds prior to cleavage development.

In the eastern part of outcrop 6, at the intersection of several faults oriented at low angles to bedding, a breccia to cataclasite occurs of several decimetres wide (Fig. 5). This breccia to cataclasite is cross-cut by cleavage.

In the western part of outcrop 6, a half meter wide zone occurs containing several subvertical, N-S-trending quartz veins, of which the thickest one is ~3 cm wide (see Figs 5 & 6G). These veins are subperpendicular to bedding, and are cross-cut by cleavage. Either these veins formed as a result of burial (pre-folding, vertical loading by overlying deposits) or they formed during N-S-directed tectonic shortening. These veins are truncated by bedding-parallel faults. The seemingly reverse, bedding-parallel fault movement of ~1.5m, as suggested by the local re-occurrence of these veins, opposes the asymmetry of the small-scale folds. However, as no fault striations are observed, this apparent displacement should be approached with caution.

4. Interpretation

4.1. Overall structure

On the basis of the orientation of cleavage and the regular bedding (i.e. bedding attitude ignoring the small-scale folds), and taking into account the quite significant regional plunge (21° towards 100°; Fig. 3 & Table 1), a traverse from outcrop 1 to outcrop 6 can be interpreted as a traverse through a decametre- to hectometre-scale, gently plunging, moderately inclined antiform, with a stepfold geometry and a S-verging asymmetry (Fig. 7). Outcrop 2 represents the steep fold limb, and outcrops 1 and 3 to 6 represent the gently dipping to subhorizontal limb. Outcrop 5, in which bedding changes from moderately S-dipping in the upper parts to steeply dipping in the lower parts, likely represents a small-scale, parasitic antiformal fold on the normal limb of the larger-scale antiform.

The reason for inferring an unobserved, possibly faulted, large-scale step fold, instead of attributing the changes in overall bedding orientation to faulting, lies in the cleavage-bedding relationship and cleavage refraction sense. In outcrop 2 on the one hand and outcrops 1, 3, 4, and 6 on the other hand, opposite senses of cleavage refraction are observed (compare Figs 4 & 5). In outcrops 1, 3, 4 and 6, looking to the east, cleavage refraction across the more competent bed shows an S-shaped pattern, whereas in outcrop 2, cleavage refraction shows a Z-shaped pattern. This change in refraction sense goes hand in hand with the change in bedding dip. Moreover, also a change in mean cleavage dip is observed between both groups of outcrops, pointing to a divergent cleavage fanning. Such a divergent cleavage fanning appears to be very common across (syn-cleavage) folds within the Abbaye de Villers Formation (e.g. Beckers & Debacker , 2006; cf. Beckers, 2003, 2004).

The opposing senses of cleavage refraction, the divergent cleavage fanning and the fact that the cleavage plots on the best fit girdle through the poles to regular bedding of outcrops 1 to 6, and approximately bisects the fold interlimb angle, all indicate that this antiform formed cogenetically with cleavage. Because of this cogenetic relationship, a tectonic origin can be concluded.

4.2. Small-scale folds

In those cases where cleavage is oblique to the fold axial surface, cross-cuts the fold axial surface and both fold limbs, and shows the same refraction sense on opposite fold limbs, a pre-cleavage fold origin can be concluded. This is the case for folds 1, 2, 6, 12, 13 and 14 (Figs 4, 5 & 6A-C). Detailed observations indicate that also folds 7, 8 and 16 show an anomalous cleavage/fold relationship and hence developed prior to cleavage development (Figs 4, 5 & 6D-E).

In the case of folds 3, 4, 5, 9, 10, 11 and 15, no clear conclusions can be drawn from the cleavage/fold relationship. Within these six folds, cleavage is at low angles to the axial surface and shows an opposing sense of cleavage refraction on opposite fold limbs (Figs 5, 6D & 6F). In addition, occasionally cleavage even shows a slightly divergent fanning across these folds. As pointed out by Debacker *et al*. (2006), also pre-cleavage folds may show a divergent fanning and opposing senses of cleavage refraction on opposite fold limbs, provided that cleavage is at very low angles to the axial surface of the pre-cleavage folds. Hence, these folds may have a pre-cleavage origin or may have a syn-cleavage origin. However, considering the similar size, asymmetry and orientation as compared to the other small-scale folds, and the fact that also these six folds are bounded above and/or below by relatively undeformed regular bedding, we interpret also these folds as having formed prior to cleavage development.

4.3. Faults

Two groups of faults can be distinguished. A first group, only observed in outcrop 2, consists of moderate to steep faults with a dip-slip movement and with a marked outcrop appearance (damage zone, depression in outcrop face). The much more common second group, oriented at low-angles to bedding, commonly being associated with pre-cleavage folds, and often having a welded nature, was observed in particular in outcrops 3, 4 and 6. This group was observed to a lesser extent also in outcrop 2, where they are often difficult to distinguish from faults of the first group. The consistently low angle with bedding allows referring to these faults as detachments.

On their own, the spatial and geometric relationship of the second group of faults (detachments) with the pre-cleavage folds (i.e. separating pre-cleavage folds from relatively undeformed underlying and/or overlying beds, fold hinge lines situated within the fault plane; e.g. see Figs 5, 6A, 6B, 6D & 6F) are no convincing arguments for a pre-cleavage fault origin. However, the fact that some of these detachments show the same curvature as the overlying pre-cleavage folds and the fact that some of these detachments are accompanied by zones of pre-cleavage breccia or cataclasite clearly indicate a pre-cleavage fault origin (Fig. 5). In turn, bearing in mind the spatial and geometric relationship with the pre-cleavage folds, it is likely that the pre-cleavage folds and the second group of faults (detachments) formed simultaneously.

Because of the combination of their outcrop appearance, the absence of any relationship with the pre-cleavage folds and the fact that they locally truncate faults of the second group (e.g. Fig. 4), the faults of the first group, thus far only observed in outcrop 2, must have formed later than those of the second group. These faults are considered to have formed after cleavage development.

4.4. Origin of the small-scale folds and related features

The pre-cleavage folds and pre-cleavage faults (detachments/faults of the second group) either formed during an older, thus far unknown, pre-cleavage tectonic deformation phase, or are a result of slumping (cf. Debacker *et al*., 2001). In the study area, as well as in the

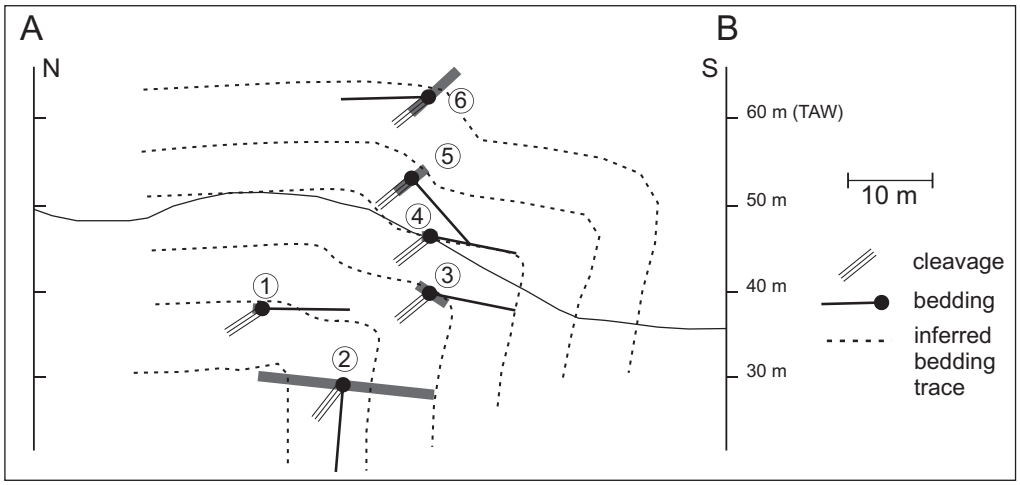

Figure 7: Vertical cross-section across the study area, showing the relative position of the beds in the six outcrops, taking into account a regional syn-cleavage fold plunge of 21° to the east (21/100). See Fig. 2 for position of section line. Grey thick lines schematically represent the projected position of the outcrops on the section.

Outcrop	Fold	Mean regular bedding	Fold B-axis	Fold axial surface	Untilted fold B-axis	Untilted axial surface	Unfolded fold -axis	Unfolded axial surface
2	1	284/85N (n=47)	07/288 (n=13)	111/70S	28/298	117/75S	13/249	241/27NW
2	2		17/100 (n=6)	079/40S	04/280	106/37S	00/096	276/59N
3	3	066/13S (n=2)	01/079 (n=4)	261/28N	19/258	234/40N	12/254	245/53NW
3	4		01/083 (n=4)	265/32N	19/262	240/42N	13/257	249/56NW
3	5		07/247 (n=6)	234/28NW	24/244	217/45NW	13/239	229/54NW
4	6	032/28SE (n=8)	14/182 (n=9)	039/25SE	10/178	094/12S	01/358	047/02SE
6	7	008/16E (n=14)	13/092 (n=6)	300/30NE	08/272	262/30N	07/271	264/35N
6	8		21/089 (n=3)	297/40NE	00/090	271/39N	01/090	272/44N
6	9		16/096 (n=4)	297/38NE	05/276	269/37N	05/276	270/42N
6	10		24/096 (n=4)	298/50NE	03/096	279/47N	03/096	279/52N
6	11		05/053 (n=4)	/	09/232	/	05/232	/
6	12		02/069 (n=6)	258/13N	16/248	216/28W	13/247	224/30NW
6	13		12/057 (n=9)	034/29SE	04/238	073/13S	01/238	058/09SE
6	14		13/069 (n=7)	064/69S	05/250	073/58S	02/250	071/54S
6	15		23/078 (n=3)	/	03/080	/	05/080	/
6	16		35/088 (n=8)	303/51NE	14/090	285/46N	15/091	285/51N

Table 2: Restoration of the pre-cleavage fold axes and pre-cleavage fold axial surfaces to their initial orientation prior to tectonic syn-cleavage deformation. This is done by removing the plunge of the overall syn-cleavage fold axis ("untilting": +21° rotation around 00/190), followed by an unfolding around the overall syn-cleavage fold axis restored to horizontal (00/100). Unfolding angles are controlled by the mean regular bedding, and values used for this are -96° for outcrop 2, -17° for outcrop 3, -11° for outcrop 4 and -05° for outcrop 6. Rotation convention: negative (positive) is anticlockwise (clockwise) when viewed downplunge.

other outcrop areas of the Brabant Massif, there is no evidence for more than one tectonic deformation phase (e.g. Sintubin, 1997, 1999; Debacker, 2001; Verniers *et al*., 2002; Debacker *et al.*, 2001, 2005, 2006, and references therein). In contrast, the pre-cleavage folds have characteristics commonly attributed to slump folds. These are the isolated, intraformational position between non-folded beds, the truncation of folds by overlying, younger

beds, the dispersed orientation of the fold axes, the often irregular fold shape, the association with other soft-sediment deformation features such as detachments, welded faults, pre-cleavage breccias and disrupted sediments, and the absence of fold-related veins or cleavage (cf. Jones, 1939; Kuenen, 1949; Helwig, 1970; Corbett, 1973; Woodcock, 1976a; Rupke, 1976; Elliott & Williams, 1988). Moreover, also in other places in the Brabant Massif, many late Early to Middle Ordovician slump folds have been encountered (e.g. Michot, 1977; Debacker, 2001; Debacker *et al*., 2003; Beckers, 2003, 2004; Beckers & Debacker, 2006). For these reasons, the pre-cleavage folds are interpreted as slump folds and the faults of the second group are interpreted as slump-related detachments.

The displaced, pre-cleavage quartz veins in outcrop 6 may seem difficult to reconcile with a slump origin of the second group of faults, as one would expect the deposits to have become lithified before quartz vein development. However, apart from the fact that lithification is not a necessity for vein development and that, depending on composition, quartz veins may form at shallow burial depths (e.g. Maltman, 1994), it is not unlikely that during later tectonic deformation some pre-existing pre-cleavage detachments with a suitable orientation got reactivated. During syn-cleavage tectonic folding, flexural slip may have occurred along pre-existing, slump-related detachments, reactivating these and displacing post-slumping, pre-cleavage quartz veins. Alternatively, during initial tectonic shortening, thrust faults may have developed along pre-existing pre-cleavage detachments.

In the light of a slump origin of the pre-cleavage folds and faults (detachments), the high concentration of pre-cleavage folds and faults and the imbricate nature some of the pre-cleavage faults (e.g. outcrop 6, Fig. 5) suggests that at least part of the observed sequence represents a contractional zone of a slump sheet. In this respect, the opposite asymmetry of folds 13 and 14 may be attributed to back-thrusting or back-folding during slump arrest against a buttress (cf. Strachan & Alsop, 2006) or may result from fold overturning of initially Z-shaped asymmetrical folds (looking east) during slump propagation and/or slump arrest.

4.5. Slump direction and palaeoslope estimate

Several methods exist for deducing palaeoslope orientation on the basis of slump fold data. All of these methods have their specific advantages and draw-backs and for this reason as many methods as possible should be used (Woodcock, 1979; Strachan & Alsop, 2006). For the data presented in this paper, four methods are used. These are the mean axis method, the separation arc method, the axial surface intersection method and the fold interlimb fold azimuth method (Fig. 8). For more detail on the advantages and disadvantages of these methods the reader is referred to Woodcock (1979) and Strachan & Alsop (2006) and references therein.

For each of the methods, slump fold data (fold axes, axial surfaces,…) have to be restored to their probable orientation prior to tectonic, cleavage-related folding. In order to do so, two consecutive rotations are performed. In the first rotation, referred to herein as untilting, the plunge of the regional, syn-cleavage fold axis (21/100; see Table 1) is removed. In the second rotation, referred to herein as unfolding, the untilted limbs of the syn-cleavage fold are unfolded (i.e. restored to horizontal) around the untilted syn-cleavage fold axis (00/100). For untilting, the same values are used for all outcrops, i.e. a rotation of 21° around 00/190. For unfolding, the same rotation axis is used for all outcrops (00/100), but with different rotation values. These rotation values depend on the mean regular bedding within each outcrop after untilting (see Tables 1 and 2).

Mean axis method

The mean axis method, proposed by Jones (1939; see also Hahn, 1913) is based on the assumption that slump fold axes statistically are parallel to the strike of the palaeoslope and perpendicular to the slump direction. The sense of slumping and palaeoslope dip sense can then be inferred from regional constraints (e.g. Jones, 1939) or from fold vergence (e.g. Crimes, 1970, Woodcock, 1976b). Importantly, this method relies on the average fold distribution (Woodcock, 1979). For our data, the mean axis method gives a mean slump fold axis with azimuth of 077° +/- 021° (Fig. 8A). Taking into account the dominant south-verging fold asymmetry, this suggests a slump direction towards 167° +/- 021°. It should be taken into account that one fold hinge line in outcrop 4 has a markedly different orientation and hence may affect the overall result. If this fold were taken out, the mean axis would be 078° +/- 015°, suggesting slumping towards 168° +/- 015° (Fig. 8A). Although the uncertainty (circular standard deviation) is much smaller, the results are, however, very similar. The reason for this primarily lies in the fact that this method relies on average distributions and is therefore quite robust (Woodcock, 1979).

Separation arc method

The separation arc method, initially proposed by Hansen (1965, 1967), is based on the observation that, during downslope translation, slump folds will tend to rotate towards the slump direction, away from the strike of the palaeoslope (cf. Lajoie, 1972). This results in folds with opposite asymmetry, ideally symmetrical about the slump transport direction. The method relies on slump fold axes orientation and fold asymmetry (looking down-plunge). It consists of outlining fields with similar down-plunge slump fold asymmetry on an equal area projection, and constructing the bisector of a "separation arc" or "separation angle" (Hansen, 1965; Wheeler, 1975) between fields with opposing down-plunge slump fold asymmetry. This separation arc or angle is a segment of the best-fit girdle through the fold axes, which in turn approaches the shear plane. Importantly, as pointed out by Woodcock (1979), the method is strongly dependent on the extreme values, rather than on average values.

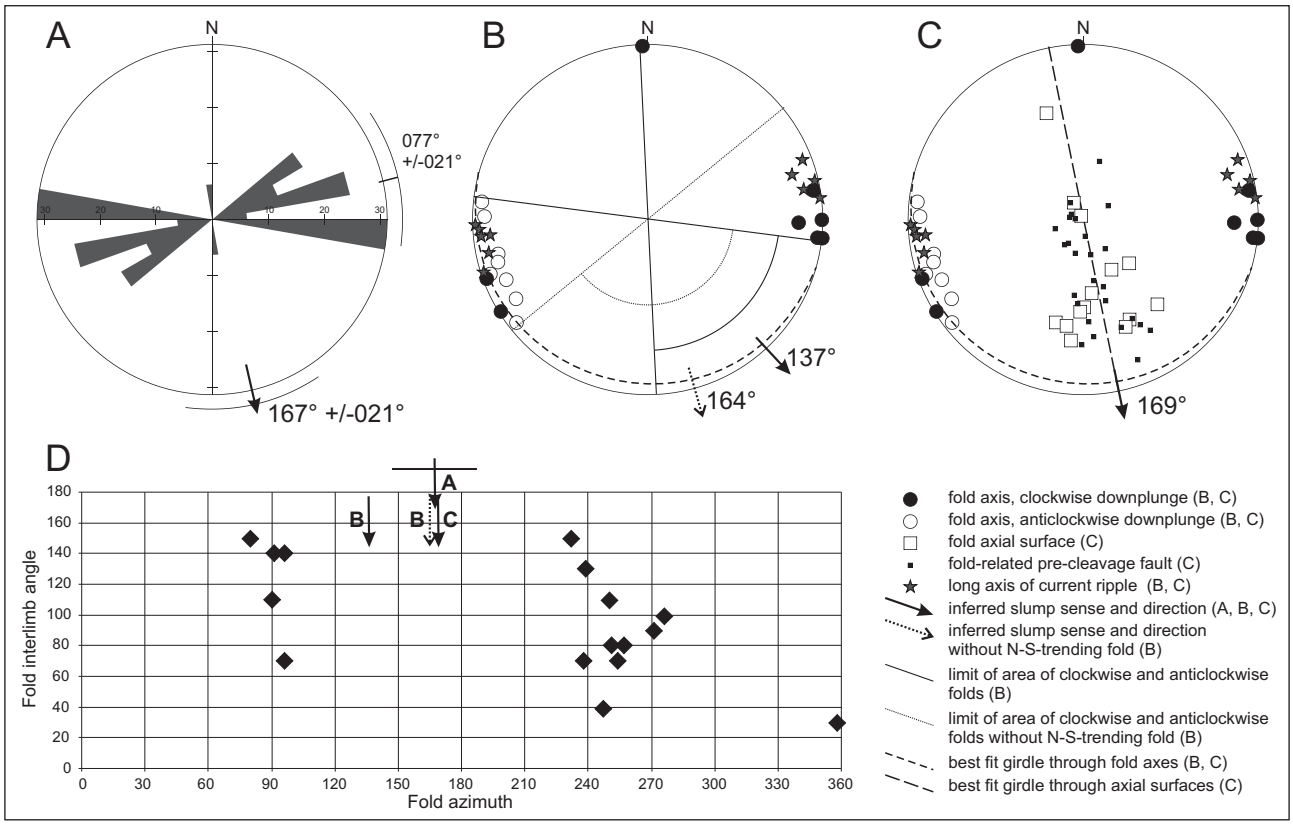

Figure 8: Determination of the slump direction on the basis of slump fold data with mean regular bedding restored to horizontal by means of an untilting of and unfolding around the overall syn-cleavage fold axis (see also Table 2): A) mean axis method (rose plot with trends of slump fold axes; sector size 10°, maximum 31.3%); B) separation arc method (lower-hemisphere equal area projection of clockwise and anticlockwise slump fold axes; current ripple long axes for reference); C) axial-planar intersection method (lower-hemisphere equal area projection of slump fold axial surfaces; poles to faults, clockwise and anticlockwise slump fold axes and current ripple long axes for reference); D) fold hinge azimuth and interlimb angle method (results of A, B and C indicated for comparative purposes). See text.

On the stereographic projection depicted in Fig. 8B, two folds occur with a clockwise asymmetry in the anticlockwise field. These two folds are folds 13 and 14 of outcrop 6, both indicating a N-vergent asymmetry. Folds with upslope vergence are not uncommon in slump sheets (Woodcock, 1976a; Blay *et al*., 1977; Strachan & Alsop, 2006), and may be due to back-thrusting or back-folding (Strachan & Alsop, 2006). In our opinion, this is also what happens in the case of folds 13 and 14. These folds are the two southeasternmost folds, occur directly above a subhorizontal pre-cleavage fault, and cause an oversteepening of bedding towards the west. Hence, for the application of the separation arc method, the asymmetry of these folds is ignored. If we take into account all folds, the separation arc suggests a slump direction towards 137° (Fig. 8B). However, as outlined above, the separation arc method is strongly influenced by the fold axes with extreme orientation values, in our case this being the fold in outcrop 4. If we were to leave out the N-S-trending fold of outcrop 4, a slump direction towards 164° would be suggested by the separation arc method, very similar to that obtained by means of the mean axis method.

Axial-planar intersection method

As pointed out by Woodcock (1979; cf. 1976a, b), slump fold axial surfaces form a maximum dispersed about the mean slump fold axis. Moreover, the mean axial surface is usually imbricated with respect to the slump sheet, dipping in the opposite direction of the palaeoslope, and can as such be used to indicate palaeoslope sense where fold asymmetry data are ambiguous (Woodcock, 1979). Despite these early observations and strong urge for the standard use of axial surfaces in the analysis of slump folds, the axial-planar intersection method was first developed by Alsop & Holdsworth (2002) for mid crustal shear zones, and was only applied to slump folds for the first time by Strachan & Alsop (2006). This method relies on the fact that layer-parallel shear should result in a fanning of the axial surfaces about the strike of the palaeoslope (Strachan & Alsop, 2006).

For our data, the axial surfaces fan about 01/079, and are generally moderately N-dipping, suggesting a slump transport towards 169° (Fig. 8C). Three axial surfaces have different dips. Two of these are from folds 13 and 14 with opposite vergence, already discussed above (see also Table 2). The third, with an orientation of 047/02SE, belongs to fold 6 of outcrop 4. This fold has an orientation at high angles to the other slump folds and close to the inferred slump direction. As pointed out by Woodcock (1979), for folds with a downslope (mean) axis, such as

fold 6, the axial plane should be close to the mean slump sheet attitude rather than imbricated. Indeed, this appears to be exactly what we observe.

On the same plot, we also added the orientation of untilted and unfolded pre-cleavage faults (second group of faults/detachments). The data points plot in exactly the same area as the axial surfaces, suggesting that these faults may indeed be related to slumping (Fig. 8C). Moreover, this seems to suggest that the vast majority of these faults have a reverse sense of movement, something which was not always apparent in outcrop. Together with the slump folds, these observations underline the contractional nature of the studied part of the slump sheet, as deduced above.

Fold hinge azimuth and interlimb angle method

This method, first applied to slump folds by Strachan & Alsop (2006), relies on the assumption that with applied shear stress folds tighten as they rotate from an original palaeoslope strike-parallel orientation to a transport-parallel orientation. On a graph of interlimb angle versus fold hinge line azimuth, such as depicted in Fig. 8D, a slump mass that has undergone no fold axis rotation will plot as two separate fields approximating the palaeoslope strike. In contrast, a slump mass that has undergone significant fold axis rotation will result in a V-shaped pattern with the apex approximating the palaeoslope dip direction (Strachan & Alsop, 2006).

As depicted on Fig. 8D, on its own this method does not allow drawing conclusions from our data set. This can be attributed partly to the scarcity of data, partly to the scarcity of downslope slump fold axes, and partly to the fact that the majority of our slump folds did not experience a significant fold axis rotation during slumping. However, a comparison with the previous methods (arrows labelled A, B, C) shows that the fold hinge azimuth and interlimb angle method is fully compatible with the results of the mean axis method, the separation arc method and the axial-planar intersection method. This particularly concerns the small interlimb angles of fold 6, being close to the slump direction, with respect to the predominantly large interlimb angles for the folds at high angles to the slump direction.

5. Discussion

5.1. Implications for Ordovician basin geometry and stratigraphy

Although situated almost 30 km along strike from the slump folds in the vicinity of the Abbey of Villers in the Thyle valley, described by Beckers (2003, 2004; cf. Beckers & Debacker, 2006; see Fig. 1), also the slump features in the Senne valley at Quenast point to a S-dipping palaeoslope. Both are compatible with the late Early to Middle Ordovician slump fold geometries within the Sennette valley at Virginal (Debacker, 2001; Debacker *et al*., 2003; see Fig. 1 for location). The fact that at the three observation points studied thus far, all slump folds point to a roughly south-directed palaeoslope, has important implications for the late Early to Middle Ordovician basin geometry of the Brabant Basin. The observations suggest that this S-directed palaeoslope did extend for at least 30 km, and therefore should not be regarded as a local phenomenon, but instead as a regionally significant phenomenon. Hence, at least during parts of the late Early to Middle Ordovician, a S-dipping regionally persistent palaeoslope existed in these parts of the Brabant Basin. Moreover, the geometric relationship of the inferred palaeoslope with the current ripple orientation suggests a close relationship between the inferred S-dipping palaeoslope and the palaeocurrent.

Interestingly, Beckers (2003, 2004) demonstrated that in the lowermost Ordovician Chevlipont Formation in the Thyle valley, directly underlying the Abbaye de Villers Formation, slump folds point to a N-dipping palaeoslope, similar to that classically inferred for the Ordovician and Silurian in the Brabant Basin (Verniers, 1983; Verniers & Van Grootel, 1991; Louwye *et al*., 1992; Verniers *et al*., 2002; Vanmeirhaeghe, 2006, Debacker & Vanmeirhaeghe, 2007; cf. Debacker *et al*., 2001). Considering that, during the time hiatus between the Chevlipont Formation and the Abbaye de Villers Formation (Verniers *et al*., 2001) the microcontinent Avalonia rifted away from Gondwana (Verniers *et al*., 2002), it is tempting to relate the discrepancy in inferred palaeoslope between the Chevlipont Formation on the one hand and the late Early to Middle Ordovician on the other hand to this event. However, it should be realised that, although the S-directed palaeoslope during the late Early to Middle Ordovician cannot be regarded any more as a local phenomenon, the same cannot be said for the Chevlipont Formation, in which, at present, only one slump fold occurrence has been studied in detail in outcrop (Beckers, 2003, 2004).

According to the new geological maps (Herbosch & Lemonne, 2000 and Herbosch *et al*., in press) the slump folds described by Debacker (2001; Debacker *et al*., 2003) and Beckers (2003, 2004; Beckers & Debacker, 2006) occur within the Abbaye de Villers Formation, whereas those described in the present study occur within the lower part of the Tribotte Formation. As shown in Beckers & Debacker (2006), the slump folds in the Thyle valley occur in a very specific part of the Abbaye de Villers Formation, being a ~10 m thick zone (or more, if extending into deeper levels), situated approximately 75 m below the base of the Tribotte Formation and, judging from the map of Herbosch & Lemonne (2000) at~44 m above the top of the Chevlipont Formation. The slump fold level described by Debacker (2001; Debacker *et al*., 2003) at Virginal in the Sennette valley is ~34 m thick and occurs at ~70 m above the top of the Chevlipont Formation and at least ~28 m below the fault-bounded contact with the (missing) Tribotte Formation and the overlying Rigenée Formation (Beckers & Debacker, 2006; Debacker *et al*., 2003; Debacker, 2001). Although admittedly there is a large uncertainty (up to several tens of meters, Herbosch, pers. comm.) regarding the exact limit between the Abbaye de Villers Formation and the Tribotte Formation, it is not impossible that the slump folds described by Beckers

(2003, 2004; Beckers & Debacker, 2006) in the Thyle valley and those described by Debacker (2001; Debacker *et al*., 2003) in the Sennette valley belong to the same stratigraphic level and correspond to the same slumping event. However, according to the geological map of Herbosch *et al*. (in press), the slump folds described within the present study occur within the Tribotte Formation. At present, without additional data, three different possible explanations may be suggested for this, all being compatible with a regionally S-dipping palaeoslope during the late Early to Middle Ordovician.

As a first possibility, it is suggested that the slump horizon of the present study is not the same horizon as that described by Beckers (2003, 2004; Beckers & Debacker, 2006) and Debacker (2001; Debacker *et al*., 2003). This implies different slumping events during the late Early to Middle Ordovician, all on a regionally S-dipping palaeoslope. As a second possibility, the lithostratigraphical attribution by Herbosch *et al*. (in press) of the outcrops under study may be incorrect, in which case the slump fold level(s) might correspond roughly to those described by Beckers (2003, 2004; Beckers & Debacker, 2006) and Debacker (2001; Debacker *et al*., 2003). As a third possibility, one should take into account the possibly diachronic nature of both the Abbaye de Villers Formation and the Tribotte Formation. The deposits of both formations are considered to have been deposited in a rather shallow environment, ranging from the mid to the inner shelf (Herbosch, pers. comm.; Vanmeirhaeghe, 2006), in which lateral facies changes and a diachronic nature cannot be ruled out. Indeed, both for the Abbaye de Villers Formation and the Tribotte Formation, lateral facies changes have been suggested previously (Herbosch & Lemonne, 2000; Herbosch, pers. comm.). In such a case, it might be possible that the slump folds described herein and those described by Beckers (2003, 2004; Beckers & Debacker, 2006) and Debacker (2001; Debacker *et al*., 2003) roughly correspond to the same slumping events, but that the Abbaye de Villers Formation and the Tribotte Formation are diachronic, seemingly becoming older towards the WNW. Although the second and third possibility may seem far fetched, without evidence showing otherwise all three possibilities should be taken into account in further studies.

5.2. Cause of slumping

For slumping to occur basically three conditions have to be fulfilled. These are a slope, weak sediments (i.e. having low shear strength) and some kind of trigger mechanism. Sediment strength is mainly controlled by lithology (grain-size, mineralogy and consolidation) and pore fluid pressure. Trigger mechanisms cause a sudden decrease in slope stability, either by increasing the shear stress acting along the slope or by decreasing the sediment strength. An increase in shear stress acting along the slope may result from the addition of an extra load on the upper parts of the slope or by the removal of a load from the bottom parts of the slope, whereas, for a given lithology, sediment strength is reduced directly by temporarily increasing the pore fluid pressure (e.g. Maltman, 1994).

The relatively coarse-grained nature of the deposits suggests fairly rapid deposition, which may result in rather unstable, fluid-overpressured deposits with low shear strength. However, considering the total absence of fluid escape structures such as dish structures, convolute bedding, pipe-structures, sand dykes, sand volcanoes…, fluid escape during deposition and burial must have been able to keep up with loading. This makes burial-induced fluid overpressuring unlikely. The scarcity of thick mudstone levels, acting as seals for fluid escape, is compatible with this deduction. Hence, the main conditions for slope failure are not fulfilled, and therefore an external trigger is needed.

As an external trigger we invoke seismic activity related to normal faulting. During the time hiatus between the Chevlipont Formation and the Abbaye de Villers Formation (Verniers *et al*., 2001) Avalonia rifted away from Gondwana (Verniers *et al*., 2002). As suggested by Verniers *et al*. (2002), this separation may be responsible for the apparent time hiatus between both formations. The much more shallow deposition environment of the Abbaye de Villers Formation and the overlying Tribotte Formation as compared to the deeply deposited, turbiditic Chevlipont Formation (e.g. Verniers *et al*., 2001) may well be a direct consequence of the upheaval of rift shoulders related to the separation of Avalonia from Gondwana. In addition, this separation must have been accompanied by normal faulting, causing seismic loading of the upper Lower to Middle Ordovician sediments and occasionally resulting in wide-spread slope failure, giving rise to the slump features documented in this study and in Debacker (2001; cf. Debacker *et al*., 2003) and Beckers (2003, 2004; cf. Beckers & Debacker, 2006). Moreover, within this rifting/oceanic separation context, both N- and S-dipping palaeoslopes can be expected. Slumping along S-dipping palaeoslopes, as inferred in this study and in the study of Beckers (2003, 2004), may be attributed to bed-parallel slumping along beds tilted due to the activity of antithetic (N-dipping) lystric normal faults, to slumping along synthetic (S-dipping) normal fault scarps, or may have occurred in small, shallow sub-basins in between syn- and antithetic rifting-related normal faults. This normal faulting generated the seismic loading responsible of lowering the sediment shear strength, and may also have increased the slope angle, adding an extra stress to the shear stresses already acting on the sediments, thus resulting in wide-spread S-directed slope failure.

6. Conclusions

The small-scale folds and the related detachments within the upper Lower to Middle Ordovician directly north of the Quenast plug are interpreted as slump features. The combined use of the mean axis method, the separation arc method, the axial-planar intersection method and to a lesser extent the fold hinge line azimuth and interlimb

angle method indicate slumping along a SSE-dipping palaeoslope. This inferred slump direction is at high angles to current ripples. Moreover, these results are fully compatible with the results of two previous studies on late Early to Middle Ordovician slump folds from other outcrop areas of the Brabant Massif (Debacker, 2001; Beckers, 2003, 2004). Together, these results point to the presence of a regionally persistent, roughly S-dipping late Early to Middle Ordovician palaeoslope in the southern part of the Brabant Massif, with an along-strike length of at least 30 km. This palaeoslope not only controlled slumping but also affected current directions. Slumping is attributed to seismic activity related to normal faulting accompanying the separation of Avalonia from Gondwana, and also the palaeoslope may be a direct consequence of this normal faulting.

Such a regional S-dipping palaeoslope in this part of the Brabant Basin is not reflected by the Upper Ordovician and Silurian geological record. The N-directed turbidity currents within the Ittre Formation (Brabant Massif; Debacker *et al*., 2001), the N-verging slump folds in the Ombret Formation (Condroz Inlier; Valcke, 2001; Valcke & Debacker, 2002), and the much more proximal nature of the turbidites of the Ombret Formation with respect to their lateral equivalents in the Ittre Formation (Vanmeirhaeghe, 2001; Vanmeirhaeghe & Verniers, 2002; Vanmeirhaeghe, 2006) all point to a regional N-dipping palaeoslope during the late Sandbian to Katian (Caradoc). Moreover, also the middle Darriwilian to Sandbian (Llanvirn to Middle Caradoc) Rigenée Formation (Brabant Massif) is characterised by deeper depositional depths as compared to its lateral equivalents within the Condroz Inlier (Vanmeirhaeghe, 2001; Vanmeirhaeghe & Verniers, 2002; Vanmeirhaeghe, 2006), again suggestive of a N-dipping regional palaeoslope. This further supports the idea that the S-dipping late Early to Middle Ordovician palaeoslope is entirely related to the rifting between Avalonia and Gondwana.

7. Acknowledgements

We kindly acknowledge Nigel Woodcock and Alain Herbosch for thoroughly reviewing the manuscript. We would also like to thank Alain Herbosch for the helpful discussions on the stratigraphy and sedimentology of the Ordovician. T.N. Debacker is a Postdoctoral Fellow of the Fund for Scientific Research-Flanders (F.W.O.-Vlaanderen). This work forms part of previous and current research projects G.0274.99, G.0094.01 and G.0271.05 of the F.W.O.-Vlaanderen.

8. References

Alsop, G.I. & Holdsworth, R.E., 2002. The geometry and kinematics of flow perturbation folds. *Tectonophysics* 350, 99-125.

André, L., Herbosch, A., Louwye, S., Servais, T., Van Grootel, G., Vanguestaine, M. & Verniers, J., 1991. Guidebook to the excursion on the stratigraphy and magmatic rocks of the Brabant Massif, Belgium. *Annales de la Société Géologique de Belgique* 114, 283-323.

Beckers, R., 2003. *Vergelijking van de plooien in de Abbaye de Villers en Chevlipont formaties (Ordovicium) in de omgeving van de Abdij van Villers, Thyle-vallei, Massief van Brabant.* Unpublished M.Sc.-thesis, Universiteit Gent.

Beckers, R., 2004. Comparison of folds in the Chevlipont and Abbaye de Villers Formations, near the abbey of Villers, Thyle valley, Brabant Massif. *Geologica Belgica* 7, 357-359.

Beckers, R. & Debacker, T.N., 2006. Influence of slump folds on tectonic folds: an example from the Lower Ordovician of the Anglo-Brabant Deformation Belt, Belgium. *Journal of the Geological Society, London* 163, 37-46.

Blay, P., Cosgrove, J.W. & Summers, J.M., 1977. An experimental investigation of the development of structures in multilayers under the influence of gravity. *Journal of the Geological Society, London* 133, 329-342.

Corbett, K.D., 1973. Open-cast slump sheets and their relationship to sandstone beds in an Upper Cambrian flysch sequence, Tasmania. *Journal of Sedimentary Petrology* 43, 147-159.

Crimes, T.P., 1970. A facies analysis of the Cambrian of Wales. *Palaeogeography Palaeoclimatology Palaeoecology* 7, 113-170

Debacker, T.N., 2001. *Palaeozoic deformation of the Brabant Massif within eastern Avalonia: how, when and why?* Unpublished Ph.D.-thesis, Universiteit Gent.

Debacker, T.N., Dewaele, S., Sintubin, M., Verniers, J., Muchez, Ph. & Boven, A., 2005. Timing and duration of the progressive deformation of the Brabant Massif, Belgium. *Geologica Belgica* 8, 20-34.

Debacker, T.N., Herbosch, A., Sintubin, M. & Verniers, J., 2003. Palaeozoic deformation history of the Asquempont-Virginal area (Brabant Massif, Belgium). *Memoirs of the Geological Survey of Belgium* 49, 30 p.

Debacker, T.N. & Sintubin, M., 2008. The Quenast plug: a mega-porphyroclast during the Brabantian Orogeny (Senne valley, Brabant Massif). *Geologica Belgica* 11, 199-216.

Debacker, T.N., Sintubin, M. & Verniers, J., 2001. Large-scale slumping deduced from structural and sedimentary features in the Lower Palaeozoic Anglo-Brabant fold belt, Belgium. *Journal of the Geological Society, London* 158, 341-352.

Debacker, T.N. & Vanmeirhaeghe, J., 2007. Pre-Devonian, Brabantian deformation within the southern Condroz Inlier (Ruisseau des Chevreuils, Dave, Belgium). *Geologica Belgica* 10, 165-169.

Debacker, T.N., van Noorden, M. & Sintubin, M., 2006. Distinguishing syn-cleavage folds from pre-cleavage folds to which cleavage is virtually axial planar: examples from the Cambrian core of the Lower Palaeozoic Anglo-Brabant Deformation Belt (Belgium). *Journal of Structural Geology* 28, 1123-1138.

DE VOS, W., VERNIERS, J., HERBOSCH, A. & VANGUESTAINE, M., 1993. A new geological map of the Brabant Massif, Belgium. *Geological Magazine* 130, 605-611.

ELLIOTT, C.G. & WILLIAMS, P.F., 1988. Sediment slump structures: a review of diagnostic criteria and application to an example from Newfoundland. *Journal of Structural Geology* 10, 171-182.

HAHN, F., 1913. Untermeerische gleitung bei Trenton falls (Nord-America) und ihr Verhaltnis zu ahnlinchen storungsbildern. *Neues Jahrbuch Mineralogie, Beilage Bd.* 36, 1-41.

HANSEN, E., 1965. Methods of deducing slip-line orientations from the geometry of folds. *Year Book of the Carnegy Institute Washington* 65, 387-405.

HANSEN, E., 1967. Natural slip folds in which the fold axes nearly parallel the slip lines. *Year Book of the Carnegy Institute Washington* 66, 536-538.

HELWIG, J., 1970. Slump folds and early structures, northeastern Newfoundland Appalachians. *Journal of Geology* 78, 172-187.

HERBOSCH, A., DUMOULIN, V., BLOCKMANS, S. & DEBACKER, T. (in press). Carte Rebecq-Ittre n° 39/1-2, Carte géologique de Wallonie, échelle 1/25000. Ministère de la Région Wallonne, Namur.

HERBOSCH, A. & LEMONNE, E., 2000. *Carte Nivelles-Genappe n° 39/7-8, Carte géologique de Wallonie, échelle 1/25000.* Namur: Ministère de la Région Wallonne.

HERBOSCH, A., VANGUESTAINE, M., DEGARDIN, J.M., DEJONGHE, L., FAGEL, N. & SERVAIS, T., 1991. Etude lithostratigraphique, biostratigraphique et sédimentologique du sondage de Lessines (bord méridional du Massif du Brabant, Belgique). *Annales de la Société Géologique de Belgique* 114, 195-212.

JONES, O.T., 1939. The geology of the Colwyn Bay district: a study of submarine slumping during the Salopian Period. *Quarterly Journal of the Geological Society of London* 95, 335-382.

KUENEN, PH.H., 1949. Slumping in the Carboniferous rocks of Pembrokeshire. *Quarterly Journal of the Geological Society of London* 104, 365-380.

LAJOIE, J., 1972. Slump fold axis orientations: an indication of paleoslope? *Journal of Sedimentary Petrology* 42, 584-586.

LEGRAND, R., 1968. Le Massif du Brabant. *Mémoires pour servir à l'Explication des Cartes Géologiques et Minières de la Belgique* 9, 1-148.

LENOIR, J.L., 1987. *Etude cartographique, pétrographique et palynologique de l'Ordovicien inférieur du bassin de la Senne.* Unpublished M.Sc.-thesis, Université Libre de Bruxelles.

LOUWYE, S., VAN GROOTEL G. & VERNIERS, J., 1992. The stratigraphy of the type locality of the ?late Wenlock/early Ludlow Mont Godart Formation and the early Ludlow Ronquières Formation, Brabant Massif, Belgium. *Annales de la Société géologique de la Belgique* 115, 307-331.

MALTMAN, A., 1994. *The geological deformation of sediments.* Chapman & Hall, London.

MICHOT, P., 1977. L'Ordovicien de la vallée de la Thyle (Brabant): structure tectonique, stratigraphie et lithologie. *Annales de la Société Géologique de Belgique* 100, 223-231.

RUPKE, N.A., 1976. Large-scale slumping in a flysch basin, Southwestern Pyrenees. *Journal of the Geological Society of London* 132, 121-130.

SERVAIS, T., HERBOSCH, A. & VANGUESTAINE, M., 1993. Review of the stratigraphy of the Ordovician in the Brabant Massif, Belgium. *Geological Magazine* 130, 699-710.

SINTUBIN, M., 1997. Cleavage-fold relationships in the Lower Paleozoic Brabant Massif (Belgium). *Aardkundige Mededelingen* 8, 161-164.

SINTUBIN, M., 1999. Arcuate fold and cleavage patterns in the southeastern part of the Anglo-Brabant Fold Belt (Belgium): tectonic implications. *Tectonophysics* 309, 81-97.

STRACHAN, L.J. & ALSOP, G.I., 2006. Slump folds as estimators of palaeoslope: a case study from the Fisherstreet Slump of County Clare, Ireland. *Basin Research* 18, 451-470.

VALCKE, S., 2001. *Structurele opbouw van de noordrand van de Condrozstrook te Ombret.* Unpublished M.Sc.-thesis, Universiteit Gent.

VALCKE, S. & DEBACKER, T.N., 2002. Structural analysis of the northern part of the Condroz Inlier at Ombret (Belgium). *Aardkundige Mededelingen* 12, 81-84.

VAN GROOTEL, G., VERNIERS, J., GEERKENS, B., LADURON, D., VERHAEREN, M., HERTOGEN, J. & DE VOS, W., 1997. Timing of subsidence-related magmatism, foreland basin development, metamorphism and inversion in the Anglo-Brabant fold belt. *Geological Magazine* 134, 607-616.

VANGUESTAINE, M., 2008. Early and Middle Ordovician acritarchs of the Senne-Sennette river valleys (Brabant Massif, Belgium) and their stratigraphic implications. *Geologica Belgica* 11, 3-23.

VANMEIRHAEGHE, J., 2001. *Litho- en biostratigrafie met Chitinozoa en sedimentologie van het Boven-Ordovicium in de heuvel Tier d'Olne (Ombret, Condrozstrook).* Unpublished M.Sc.-thesis, Universiteit Gent.

VANMEIRHAEGHE, J., 2006. *The evolution of the Condroz-Brabant Basin from Middle Ordovician to Llandovery: lithostratigraphical and chitinozoan biostratigraphical approach.* Unpublished Ph.D.-thesis, Universiteit Gent.

VANMEIRHAEGHE, J., 2007. Review of the lithostratigraphy of the Middle Ordovician to Llandovery of the Condroz Inlier (Belgium) by Chitinozoan biostratigraphy: Does the sedimentary succession record the Ardennian deformation? *Geologica Belgica* 10, 162-164.

VANMEIRHAEGHE, J. & VERNIERS, J., 2002. Biostratigraphy with chitinozoans and lithostratigraphy of the Tier d'Olne hill (Ombret, Condroz Inlier, Belgium). *Aardkundige Mededelingen* 12, 85-88.

VERNIERS, J., 1983. The Silurian of the Mehaigne area (Brabant Massif, Belgium), lithostratigraphy and features of the sedimentary basin. *Professional Paper of the Geological Survey of Belgium* 203, 1-117.

Verniers, J. & Van Grootel, G., 1991. Review of the Silurian in the Brabant Massif, Belgium. In *Proceedings of the international meeting on the Caledonides of the Midlands and the Brabant Massif* (Brussels, 1989, L. André, A. Herbosch, M. Vanguestaine & J. Verniers, eds.). *Annales de la Société Géologique de Belgique* 114, 163-193.

Verniers, J., Herbosch, A., Vanguestaine, M., Geukens, F., Delcambre, B. Pingot, J.L., Belanger, I., Hennebert, M., Debacker, T., Sintubin, M. & De Vos, W., 2001. Cambrian-Ordovician-Silurian lithostratigraphic units (Belgium). *Geologica Belgica* 4, 5-38.

Verniers, J., Pharaoh, T., André, L., Debacker, T., De Vos, W., Everaerts, M., Herbosch, A., Samuelsson, J., Sintubin, M. & Vecoli, M., 2002. *The Cambrian to mid Devonian basin development and deformation history of Eastern Avalonia, east of the Midlands Microcraton: new data and a review.* In: J. Winchester, Pharaoh, T., Verniers, J. (eds) Palaeozoic Amalgamation of Central Europe. Geological Society, London, Special Publications 201, 47-93.

Wheeler, R.L., 1975. Kinematic tests of multiple working hypotheses for the origin of contorted zones, Marcellus Formation, eastern Plateau Province, West Virginia. *Abstracts and Program, Geological Society of America* 7, 132-133.

Woodcock, N.H., 1976a. Structural style in slump sheets: Ludlow Series, Powys, Wales. *Journal of the Geological Society of London* 132, 399-415.

Woodcock, N.H., 1976b. Ludlow Series slumps and turbidites and the form of the Montgomery Trough, Powys, Wales. *Proceedings of the Geologists Association* 87, 169-182.

Woodcock, N.H., 1979. The use of slump structures as palaeoslope orientation estimators. *Sedimentology* 26, 83-99.

Manuscript received 25.09.2008, accepted in revised form 05.01.2009, available on line 01.02.2009